

Chemical Synthesis of All Phosphatidylinositol Mannoside (PIM) Glycans from *Mycobacterium tuberculosis*

Siwarutt Boonyarattanakalin,^{†,‡} Xinyu Liu,^{†,§} Mario Michieletti,^{†,||} Bernd Lepenies,[†] and Peter H. Seeberger^{*,†}

Laboratory for Organic Chemistry, Swiss Federal Institute of Technology (ETH) Zürich, Wolfgang-Pauli-Str. 10, HCI F312, 8093 Zürich, Switzerland, and Sirindhorn International Institute of Technology, Thammasat University, P.O. Box 22 Thammasat-Rangsit Post Office, Pathumthani 12121, Thailand

Received August 8, 2008; E-mail: seeberger@org.chem.ethz.ch

Abstract: The emergence of multidrug-resistant tuberculosis (TB) and problems with the BCG tuberculosis vaccine to protect humans against TB have prompted investigations into alternative approaches to combat this disease by exploring novel bacterial drug targets and vaccines. Phosphatidylinositol mannosides (PIMs) are biologically important glycoconjugates and represent common essential precursors of more complex mycobacterial cell wall glycolipids including lipomannan (LM), lipoarabinomannan (LAM), and mannan capped lipoarabinomannan (ManLAM). Synthetic PIMs constitute important biochemical tools to elucidate the biosynthesis of this class of molecules, to reveal PIM interactions with host cells, and to investigate the function of PIMs as potential antigens and/or adjuvants for vaccine development. Here, we report the efficient synthesis of all PIMs including phosphatidylinositol (PI) and phosphatidylinositol mono- to hexa-mannoside (PIM₁ to PIM₆). Robust synthetic protocols were developed for utilizing bicyclic and tricyclic orthoesters as well as mannosyl phosphates as glycosylating agents. Each synthetic PIM was equipped with a thiol-linker for immobilization on surfaces and carrier proteins for biological and immunological studies. The synthetic PIMs were immobilized on microarray slides to elucidate differences in binding to the dendritic cell specific intercellular adhesion molecule-grabbing nonintegrin (DC-SIGN) receptor. Synthetic PIMs served as immune stimulators during immunization experiments in C57BL/6 mice when coupled to the model antigen keyhole-limpet hemocyanin (KLH).

Introduction

Tuberculosis (TB) is a complex disease and a major cause of mortality worldwide.^{1–3} Despite the development of new treatments, TB remains a global health concern.^{4,5} Annually, there are more than seven million new cases and two million deaths caused by TB.⁶ Coinfection with HIV leads to an exacerbation of the disease⁴ and contributes to higher mortality in HIV patients.^{6,7} Programs to combat TB in many countries have failed to eradicate TB,⁸ partly due to the spread of

multidrug-resistant TB⁹ and the low efficacy of the BCG vaccine. Therefore, the exploration of novel drug targets and vaccines against *Mycobacterium tuberculosis* (*Mtb*), the main causative pathogen of TB, is essential.

Among pathogenic bacteria, *Mtb* causes more deaths in humans than any other pathogen.^{6,10,11} Approximately one-third of the world population has already been infected by *Mtb*.⁴ *Mtb* is an intracellular pathogen that has evolved to persist efficiently in infected macrophages.^{4,8,12} The composition of the *Mtb* cell wall is important for the interaction with host cells during the initial steps of the infection. Later, cell wall components play a crucial role in modulating the pro-inflammatory response by macrophages and also serve as a protective barrier to prevent antituberculosis agents from permeating inside. Consequently, the antibiotics used for the treatment of tuberculosis require long-term administration.⁵ Mortality in people living in developing countries is high since their access to these antibiotics is often limited and compliance with treatment courses is low.

The major components of the mycobacterial cell wall are the mycoyl arabinogalactan-peptidoglycan (mAGP) complex and interspersed glycolipids including ManLAM, LAM, LM, and

[†] Swiss Federal Institute of Technology (ETH) Zürich.

[‡] Sirindhorn International Institute of Technology.

[§] Current address: Department of Biological Chemistry and Molecular Pharmacology, Harvard Medical School, 240 Longwood Avenue, Boston, MA 02115.

^{||} Visiting Ph.D. student from Università degli Studi del Piemonte Orientale “Amedeo Avogadro”, Novara, Italy.

(1) Koul, A.; Herget, T.; Klebl, B.; Ullrich, A. *Nat. Rev. Microbiol.* **2004**, *2*, 189–202.

(2) Boshoff, H. I.; Barry, C. E. *Nat. Rev. Microbiol.* **2005**, *3*, 70–80.

(3) McMurray, D. N.; Carlomagno, M. A.; Mintzer, C. L.; Tetzlaff, C. L. *Infect. Immun.* **1985**, *50*, 555–559.

(4) Russell, D. G. *Nat. Rev. Microbiol.* **2007**, *5*, 39–47.

(5) Sacchetti, J. C.; Rubin, E. J.; Freundlich, J. S. *Nat. Rev. Microbiol.* **2008**, *6*, 41–52.

(6) Martin, C. *Eur. Respir. J.* **2005**, *26*, 162–167.

(7) Nunn, P.; Williams, B.; Floyd, K.; Dye, C.; Elzinga, G.; Raviglione, M. *Nat. Rev. Immunol.* **2005**, *5*, 819–826.

(8) Russell, D. G. *Nat. Rev. Mol. Cell. Biol.* **2001**, *2*, 569–577.

(9) Sharma, S. K.; Mohan, A. *Chest* **2006**, *130*, 261–272.

(10) Malin, A. S.; Young, D. B. *BMJ* **1996**, *312*, 1495.

(11) Sharma, S. K.; Mohan, A.; Indian, J. *Med. Res.* **2004**, *120*, 354–376.

(12) Hoppe, H. C.; de Wet, B. J.; Cywes, C.; Daffe, M.; Ehlers, M. R. *Infect. Immun.* **1997**, *65*, 3896–3905.

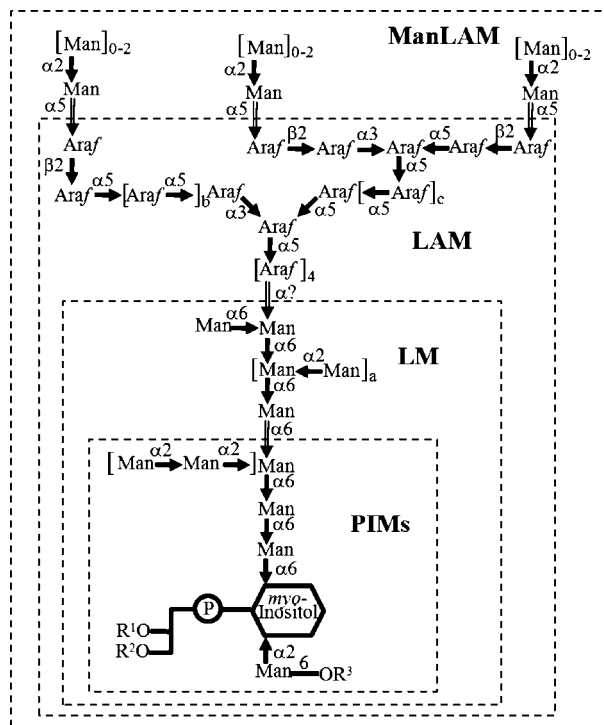


Figure 1. Structural features of PIMs, LM, LAM, and ManLAM of *Mycobacterium tuberculosis*. PIMs are the common precursors of more complex components of the mycobacterial cell wall including lipomannan (LM), lipoarabinomannan (LAM), and mannan capped lipoarabinomannan (ManLAM). (a, b, and c are varied; typically, R² is tuberculostearic acid, R¹ and R³ are various fatty acids.)

PIMs. While the mAGP complex is covalently attached to the bacterial plasma membrane, the glycolipids are noncovalently attached through their phosphatidyl-*myo*-inositol (PI) anchor.^{13–15} PIMs constitute the only conserved substructure of LM, LAM, and ManLAM (Figure 1). The inositol residue of PI is mannosylated at the C-2 position to form PIM₁ and further at the C-6 position to form PIM₂, one of the two most abundant naturally occurring PIMs, along with PIM₆. Further α -1,6 mannosylations give rise to PIM₃ and PIM₄—the common biosynthetic precursors for PIM₅, PIM₆, and the much larger LM structures. LAM is constituted by attachment of arabinans—the repeating units of α -1,5 arabinose terminated with a single β -1,2 arabinose to mannose units of LM. The nonreducing end arabinose in the arabinan moiety of LAM can be capped at the C-5 position with one or two α -mannose units to furnish ManLAM.

Among the surface components involved in the *Mtb* interaction with host cells, PIMs play a crucial role in the modulation of the host immune response.^{16–23} The functional importance

of PIMs was emphasized by the finding that PIMs bind to receptors on both phagocytic^{17,24,25} and nonphagocytic¹² mammalian cells. Recently, it has been shown that PIMs, but neither LAM nor ManLAM interact with the VLA-5 on CD4⁺ T lymphocytes and induce the activation of this integrin.²² These findings suggest that PIMs are not only secreted to the extracellular environment, but also exposed on the surface of *Mtb* to interact with host cells.

Although different functions have been ascribed to the PIMs, it remains to be determined whether and to which extent the different PIM substructures display biological activity. A better understanding of the mycobacterial cell wall biosynthesis is required to be able to counteract with the problems of drug resistance and bacterial persistence. Synthetic PIMs represent important biochemical tools to elucidate biosynthetic pathways and to reveal interactions with receptors on host cells. PIMs are potential vaccine antigens and/or adjuvants.

Several synthetic PIMs containing fewer mannoside units have been synthesized employing various chemical methodologies.^{26–33} In contrast to PIM₃ and PIM₄ that contain only α -1,6 mannosidic linkages, PIM₅ and PIM₆ also incorporate α -1,2 mannosides that might contribute to different biological activities of these PIMs. None of the studies to date utilized synthetic PIMs that contain linkers for immobilization. Coupling of synthetic PIMs to carrier proteins, beads, quantum dots, microarray or surface plasmon resonance (SPR) surfaces opens a host of options for biochemical studies. Here, we report the efficient synthesis of the carbohydrate portion of all PIMs including phosphatidylinositol (PI) to PIM₆ (Figure 2). The native diacylglycerol phosphate at the C-1 position of *myo*-inositol is replaced by a 6-thiohexyl phosphate residue for immobilization of the synthetic PIMs on surfaces.

Results and Discussion

Retrosynthetic Analysis. The overall structure of the synthetic PIM targets (Figure 2) can be attained by the convergent union of oligomannosides with *D*-*myo*-inositol containing pseudosaccharides and a thiol-terminated phosphate linker (Scheme 1). Late-stage couplings between protected oligosaccharide fragments (1–4) and 8 allow for parallel syntheses of the intermediates for all target molecules. The key glycosylations in these syntheses are the couplings between mannosyl phosphate 1, oligomannosyl trichloroacetimidates (2–4) and the common

- (13) Brennan, P. J. *Tuberculosis* **2003**, *83*, 91–97.
- (14) Crick, D. C.; Mahapatra, S.; Brennan, P. J. *Glycobiology* **2001**, *11*, 107R–118R.
- (15) Berg, S.; Kaur, D.; Jackson, M.; Brennan, P. J. *Glycobiology* **2007**, *17*, 35–56R.
- (16) Chatterjee, D.; Khoo, K. H. *Glycobiology* **1998**, *8*, 113–120.
- (17) Villeneuve, C.; Gilleron, M.; Maridonnet-Pardini, I.; Daffe, M.; Astarie-Dequeker, C.; Etienne, G. *J. Lipid. Res.* **2005**, *46*, 475–483.
- (18) Sundaramurthy, V.; Pieters, J. *Microbes Infect.* **2007**, *9*, 1671–1679.
- (19) Apostolou, I.; Takahama, Y.; Belmant, C.; Kawano, T.; Huerre, M.; Marchal, G.; Cui, J.; Taniguchi, M.; Nakauchi, H.; Fournie, J. J.; Kourilsky, P.; Gachelin, G. *Proc. Natl. Acad. Sci. U.S.A.* **1999**, *96*, 5141–5146.
- (20) Nigou, J.; Gilleron, M.; Rojas, M.; Garcia, L. F.; Thurnher, M.; Puzo, G. *Microbes Infect.* **2002**, *4*, 945–953.

- (21) de la Salle, H.; et al. *Science* **2005**, *310*, 1321–1324.
- (22) Rojas, R. E.; Thomas, J. J.; Gehring, A. J.; Hill, P. J.; Belisle, J. T.; Harding, C. V.; Boom, W. H. *J. Immunol.* **2006**, *177*, 2959–2968.
- (23) Vliegthart, J. F. *FEBS Lett.* **2006**, *580*, 2945–2950.
- (24) Thorson, L. M.; Doxsee, D.; Scott, M. G.; Wheeler, P.; Stokes, R. W. *Infect. Immun.* **2001**, *69*, 2172–2179.
- (25) Torrelles, J. B.; Azad, A. K.; Schlesinger, L. S. *J. Immunol.* **2006**, *177*, 1805–1816.
- (26) Elie, C. J. J.; Dreef, C. E.; Verduyn, R.; Vandermarel, G. A.; Van Boom, J. H. *Tetrahedron* **1989**, *45*, 3477–3486.
- (27) Elie, C. J. J.; Verduyn, R.; Dreef, C. E.; Brounts, D. M.; Vandermarel, G. A.; Van Boom, J. H. *Tetrahedron* **1990**, *46*, 8243–8254.
- (28) Elie, C. J. J.; Verduyn, R.; Dreef, C. E.; Vandermarel, G. A.; Van Boom, J. H. *J. Carbohydr. Chem.* **1992**, *11*, 715–739.
- (29) Watanabe, Y.; Yamamoto, T.; Ozaki, S. *J. Org. Chem.* **1996**, *61*, 14–15.
- (30) Watanabe, Y.; Yamamoto, T.; Okazaki, T. *Tetrahedron* **1997**, *53*, 903–918.
- (31) Stadelmaier, A.; Schmidt, R. R. *Carbohydr. Res.* **2003**, *338*, 2557–2569.
- (32) Jayaprakash, K. N.; Lu, J.; Fraser-Reid, B. *Bioorg. Med. Chem. Lett.* **2004**, *14*, 3815–3819.
- (33) Stadelmaier, A.; Biskup, M. B.; Schmidt, R. R. *Eur. J. Org. Chem.* **2004**, 3292–3303.

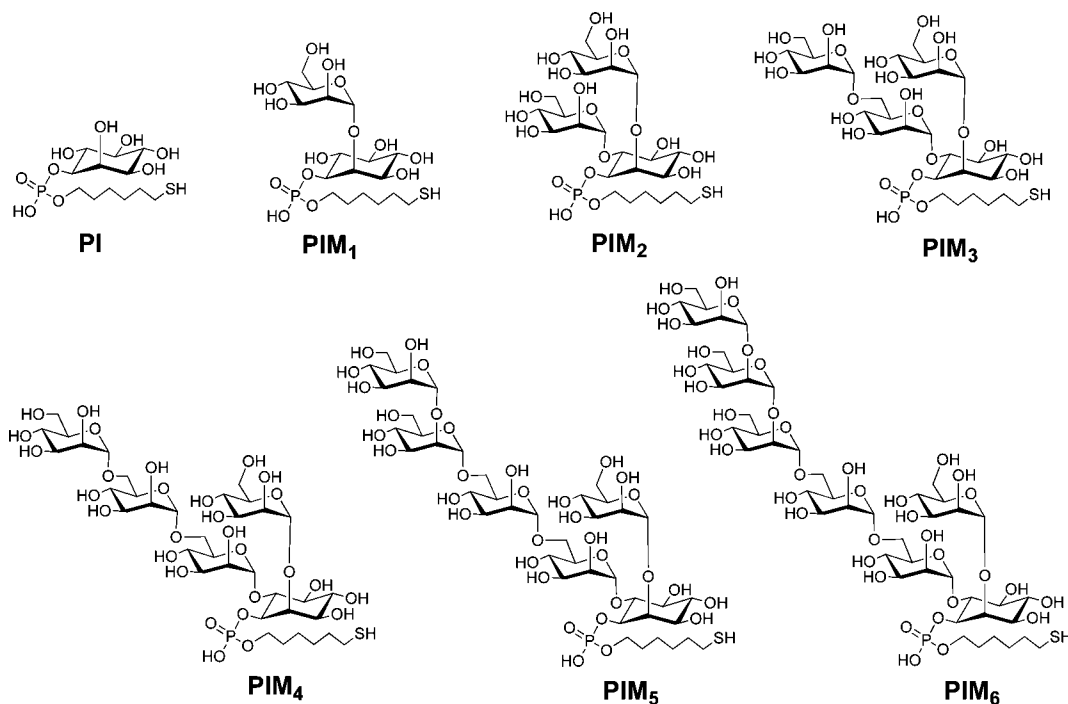
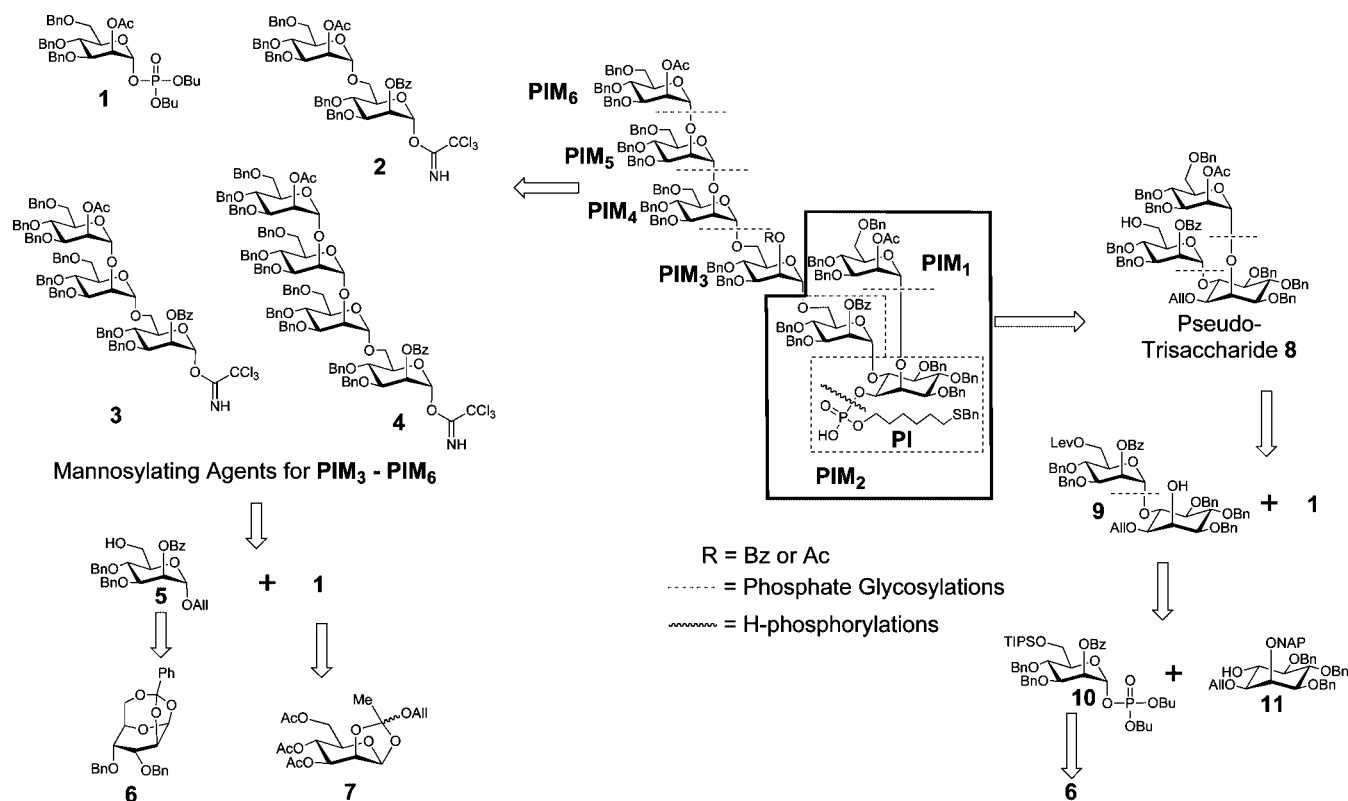


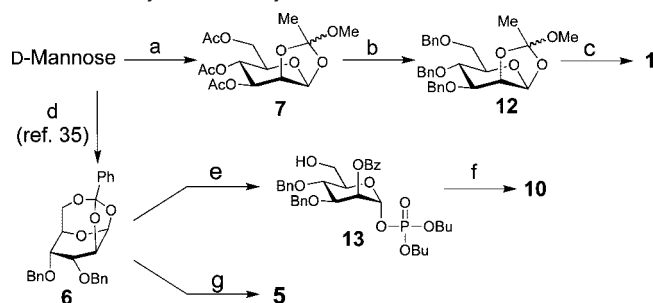
Figure 2. Structures of synthetic **PI** and **PIM₁** to **PIM₆**.

Scheme 1. Retrosynthetic Analysis for the Assembly of Synthetic PIMs

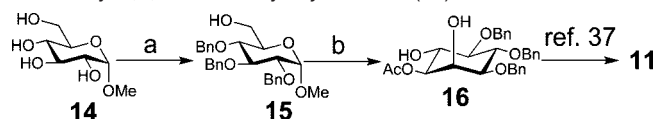


pseudotrisaccharide **8**. The two main carbohydrate moieties are coupled, followed by protecting group manipulations. Subsequently, a phosphate diester linker is installed using an H-phosphonate followed by oxidation of phosphorus. Since the target molecules contain sulfur that is known to deactivate the Pd/C catalyst, the permanent benzyl protecting groups are globally removed via Birch reduction.

The stereoselectivity of each glycosidic bond formation is ensured by neighboring C-2 acyl participating groups. In this study, we employed an anomeric dibutyl phosphate ester as a leaving group for the mannose building blocks that can be readily prepared. This method proved advantageous when compared to previous PIM syntheses. Three mannose building blocks (**1**, **5**, and **10**) are needed in addition to the inositol building block.

Scheme 2. Efficient Multi-Gram Preparations of Mannose Building Blocks via Bicyclic and Tricyclic Orthoester Intermediates^a


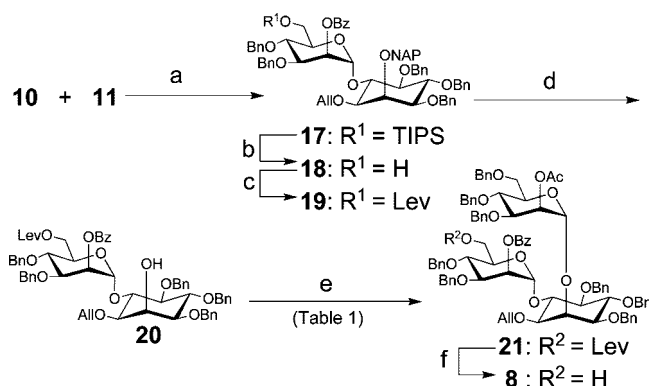
^a Reagents and conditions: (a) i. Ac₂O, HClO₄ (cat.), ii. HBr/HOAc, iii. MeOH, Lutidine, 90%, three steps; (b) i. NaOMe/MeOH/THF, ii. NaH, BnBr, DMF, quant. two steps; (c) HOP(O)(OBu)₂, 4 Å MS 93%; (d) ref 35 - i. BzCl, Py, ii. HBr/HOAc, iii. AlOH, Lutidine, iv. NaOMe/MeOH/THF, reflux, v. CSA, MeCN, vi. NaH, BnBr, DMF, 70%, six steps; (e) HOP(O)(OBu)₂, 4 Å MS, 97%; (f) TIPSCI, NEt₃, DMAP, CH₂Cl₂, 91%; (g) AlOH, BF₃·Et₂O, CH₂Cl₂, 99%.

Scheme 3. Modified Synthesis of 1-O-Acetyl-3,4,5-tri-O-benzyl-*myo*-inositol (**16**)^a


^a Reagents and conditions: (a) i. Imidazole, TIPSCI, DMF 0 °C to rt, ii. NaH, BnBr, DMF, 0 °C to rt, iii. TBAF, THF, 99%, three steps; (b) i. SO₃-Py, DIPEA, DMSO, CH₂Cl₂, 0 °C to rt, ii. K₂CO₃, Ac₂O, MeCN, reflux, iii. Hg(CF₃COO)₂, Acetone/H₂O (4:1), rt, 1 h, then NaOAc (aq), NaCl (aq), 0 °C to rt, iv. NaBH(CH₃COO)₃, AcOH, MeCN, 0 °C to rt, 40%, four steps.

Syntheses of Monosaccharide Building Blocks. Mannosyl building blocks **1**, **5**, and **10** were synthesized from mannose bicyclic and tricyclic orthoesters (**6**, **12**, Scheme 2).^{34,35} Starting from D-mannose, mannosyl phosphate **1** was accessed in six steps by dibutyl phosphoric acid opening of the bicyclic orthoester **7**. Mannosyl tricyclic orthoester **6** is readily available from D-mannose over six high yielding steps.³⁵ This process required only one purification at the last step and gave **6** in 70% overall yield. The versatile intermediate **6** was opened by allyl alcohol upon activation with BF₃·Et₂O to afford **5** in excellent yield. Treatment of orthoester **6** with dibutyl phosphate selectively opened the tricyclic orthoester to furnish glycosyl phosphate **13**, leaving the C-6 hydroxyl group unprotected. The installation of a triisopropylsilyl (TIPS) group was straightforward and furnished building block **10**.

The previously reported synthetic route to the differentially protected *myo*-inositol by Fraser-Reid et al.³⁶ was modified (Scheme 3). Methyl glucopyranose was quantitatively converted to **15** in three consecutive steps. A Parikh-Doering reaction oxidized the primary hydroxyl group in **15** to an aldehyde in quantitative yield. Using this oxidation, we avoided complications arising from the urea byproduct created when dicyclohexylcarbodiimide (DCC) was used as activator. The sulfate byproduct was readily removed by water extraction. The partially protected *myo*-inositol **16** was prepared from **15** in 40% yield over four consecutive steps. The allyl and NAP protecting

Scheme 4. Assembly of *myo*-Inositol Containing Pseudotrisaccharide **8**^a


^a Reagents and conditions: (a) TMSOTf, Toluene, -40 °C, 90%; (b) AcCl, MeOH, CH₂Cl₂, 0 °C, quant.; (c) LevOH, DIPC, DMAP, quant.; (d) DDQ, CH₂Cl₂, MeOH, 0 °C, 95%; (e) **1**, TBDMSOTf, Toluene, -40 °C, 95%, (see Table 1); (f) H₂NNH₃OAc, MeOH, rt, 89%.

Table 1. Effects of Promoter and Temperature on the Glycosylation of Glycosyl Phosphate **1** and *myo*-inositol Intermediate **20**

entry	promoter	temperature (°C)	yield (%)
1	TMSOTf	-40	15
2	TBDMSOTf	-40	27
3	TBDMSOTf	-10	57
4	TBDMSOTf	rt	55
5	TBDMSOTf	0	95

groups were introduced at C1 and C2 of the D-*myo*-inositol respectively as previously described³⁷ to furnish **11**, ready for further decoration at the C6 hydroxyl group.

Assembly of *myo*-Inositol Containing Pseudosaccharides. The *myo*-inositol containing pseudotrisaccharide **8** was assembled in a stepwise manner. Glycosylation of inositol **11** with mannosyl phosphate **10** that contained a C6-TIPS ether as a temporary protecting group was found to be optimal at -40 °C, in toluene, and promoted by a stoichiometric amount of TMSOTf (Scheme 4). Under these conditions the reaction gave a good yield with complete α-selectivity. To sustain further glycosylations, the temporary TIPS protecting group was replaced by the levulinoyl (Lev) group. The presence of TIPS rather than Lev on the C6 hydroxyl group of **10** was found necessary to balance its reactivity with inositol **10** to obtain high yield and selectivity, as observed in a previous study.³⁷ Treatment of **19** with DDQ unmasked the C2 hydroxyl group on inositol to give **20** that served in turn as nucleophile during the next mannosylation.

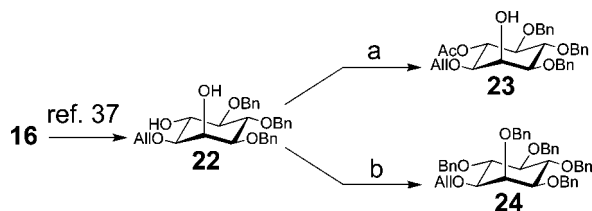
The second mannosylation on the C2 hydroxyl group of pseudodisaccharide **20** was found to be nontrivial (Table 1). Activation by TMSOTf afforded the desired pseudodisaccharide **21** in just 15% yield (Table 1, Entry 1). Decomposition of **1** to form the anomeric alcohol was observed instead. Switching the promoter from TMSOTf to the milder activator TBDMSOTf dramatically improved the yield of the desired product (Table 1, Entry 2). This observation suggested a possible reactivity mismatch between highly activated **1** and less activated **20**. The glycosylation was thus improved by reducing the reactivity of **1** with TBDMSOTf. The activity of the less reactive **20** was increased by higher reaction temperatures. Product **21** was

(34) Ravida, A.; Liu, X.; Kovacs, L.; Seeberger, P. H. *Org. Lett.* **2006**, *8*, 1815–1818.

(35) Liu, X.; Wada, R.; Boonyarattanakalin, S.; Castagner, B.; Seeberger, P. H. *Chem. Commun.* **2008**, 3510–3512.

(36) Jia, Z. J.; Olsson, L.; Fraser-Reid, B. *J. Chem. Soc., Perkin Trans. 1* **1998**, 631.

(37) Liu, X.; Stocker, B. L.; Seeberger, P. H. *J. Am. Chem. Soc.* **2006**, *128*, 3638–3648.

Scheme 5. Protecting Group Manipulations on *myo*-Inositol **16** for PI Intermediate **23** and PIM₁ Intermediate **24**^a

^a Reagents and conditions: (a) Ac₂O, DMAP, Py, 70%; (b) NaH, BnBr, DMF, 0 °C to rt, quant.

obtained in excellent yield (95%) and selectivity by performing the glycosylation at 0 °C (Table 1, Entry 5). The α linkages in **21** were confirmed by 2D NMR. ¹H–¹³C coupled HSQC NMR indicated ¹H1–¹³C1 coupling constants ($J_{C1,H1}$) of 178 Hz at the anomeric position of the mannose connected to the C2 of inositol and 182 Hz at the anomeric position of the mannose on C6 of inositol. $J_{C1,H1}$ of β mannosidic linkages are typically lower at around 159 Hz.³⁸

Removal of the Lev group in **21** was achieved by treatment with hydrazine acetate in methanol and required careful monitoring. Longer reaction times resulted predominantly in the reduction of the allyl moiety to a propyl group. Partially protected inositol **16** was subjected to protecting group manipulations to furnish the inositol intermediates for **PI** and **PIM₁** (Scheme 5). Based on reactivity differences, the equatorial C6 hydroxyl group of the diol **22** was selectively acetylated to afford **23** as the intermediate en route to **PIM₁**. The **PI** intermediate **24** was obtained in parallel by benzylation of the common intermediate **22**.

Assembly of Oligomannoside Fragments. The oligomannoside trichloroacetimidates **2**, **3**, and **4** were assembled in linear fashion (Scheme 6). All glycosylations employed mannosyl phosphate **1** and TMSOTf as activator. The α -1,6 glycosidic bond was readily formed at 0 °C in quantitative yield. A lower temperature (–40 °C) was required to efficiently install 1,2 glycosylic linkages with complete α -selectivity. Deallylation of **25**–**27** was performed by allylic substitutions mediated by a palladium complex to yield the corresponding anomeric alcohols **28**–**30**. Finally, conversion to the glycosyl trichloroacetimidates **2**–**4** was carried out using sodium hydride as base.

Assembly of Protected PIM Backbones. Prior to phosphorylation, all protected PIM oligosaccharide backbones were obtained by late-state glycosylations (Table 2). Following these glycosylations all ester protecting groups were removed with sodium methoxide in methanol at elevated temperature before masking the free hydroxyl groups as benzyl ethers. These protecting group manipulations were performed to avoid the persistence of *O*-benzoate protecting groups under Birch conditions in the final deprotection.³⁹

Coupling between mannosyl phosphate **1** and inositol **23** gave pseudodisaccharide **31**, the backbone of **PIM₁**. To access the **PIM₂** backbone, pseudotrisaccharide fragment **8** was directly used as the starting material to be transformed into backbone **32**. The glycosylation products from couplings (Table 2, entry 3–5) between the oligomannosyl trichloroacetimidates (**1**–**3**) and the common pseudotrisaccharide **8** were cleanly achieved

at –10 °C. After quenching with triethylamine, the concentrated crude products were directly converted to obtain the benzylated products. When the larger structure **4** was used for glycosylation, the coupling became more sluggish and resulted in the hydrolysis of **4**. A higher temperature (0 °C) was needed to obtain the **4** + **3** glycosylation product **46** (see Experimental Section). Pseudoheptasaccharide **46** was the largest oligosaccharide assembled in this series and consisted of fragments of all smaller oligosaccharides. Thus, **46** was analyzed extensively by C–H coupled HSQC to confirm its structural identity. 2D-NMR data elucidated six anomeric proton signals with typical³⁸ α -manno $J_{C1,H1}$ couplings.

Removal of *O*-Allyl Protecting Group on Inositol. Protocols to cleave the C-1 *O*-allyl group on inositol attached to oligosaccharides, performed by using PdCl₂, have been reported to give moderate yields.^{32,40–43} This literature precedence was reflected in our study as well. Different methods to remove the *O*-allyl group were explored on substrate **31** (Scheme 7 and Table 3). The hydrogen activated iridium complex Ir{(COD)[PH₃(C₆H₅)₂]₂}PF₆ was found to be the most efficient reagent to isomerize the allyl group to the corresponding enol ether. In the same pot, a catalytic amount of *p*-toluenesulfonic acid (*p*-TsOH) was added to cleave the enol ether and liberate the C1 hydroxyl of pseudodisaccharide **38** in quantitative yield. This two step procedure was applied to the larger oligosaccharides **32** to **36** as well. However, while the isomerizations mediated by the iridium complex worked smoothly, an excess of *p*-TsOH (10 equiv) was required to cleave the enol ether and furnish **39**–**43** (Scheme 7, entry 3).

Phosphorylation and Global Deprotection. The phosphate moiety accompanied by a terminal thiol linker was installed on the inositol C1 hydroxyl group of the oligosaccharide backbone **37**–**43** using a H-phosphonate (Scheme 8). Substrates **37**–**43** were treated with pivaloyl chloride in the presence of linker **44** and pyridine. Subsequently, in the same pot, the H-phosphonate diesters were oxidized with iodine and water to provide the fully benzylated phosphodiester **45** as triethylamine salts in excellent yield. Global removal of benzyl protecting groups of analogs **45a**–**g** was achieved under Birch reduction conditions. The fully protected compounds were treated with sodium dissolved in ammonia to furnish the final products **PI** and **PIM₁–PIM₆** (Figure 2). Small amounts of incompletely reduced products were observed containing some remaining benzyl groups. These side products were separated by extraction with chloroform and converted to the final products by resubmission to Birch reduction. The final products were formed as a mixture of monomers and disulfide dimers. Treatment with one equivalent of tris(carboxyethyl) phosphine hydrochloride (TCEP) immediately prior to conjugation of the final compounds ensured that **PI** and **PIM₁–PIM₆** were present as monomers.

PIM Microarrays to Determine Binding to DC-SIGN. To study the interactions of synthetic **PI** and **PIMs** with the protein DC-SIGN on a microarray, **PI** and **PIMs** were immobilized on a maleimide activated glass slide via their thiol handle following established protocols (Figure 3).⁴⁴ DC-SIGN is an important receptor on dendritic cells and contributes to the initiation of a pro-inflammatory response by host cells.^{45–47} One of the functions of DC-SIGN is the recognition of evolutionary

(38) Podlasek, C. A.; Wu, J.; Stripe, W. A.; Bondo, P. B.; Serianni, A. S. *J. Am. Chem. Soc.* **1995**, *117*, 8635–8644.

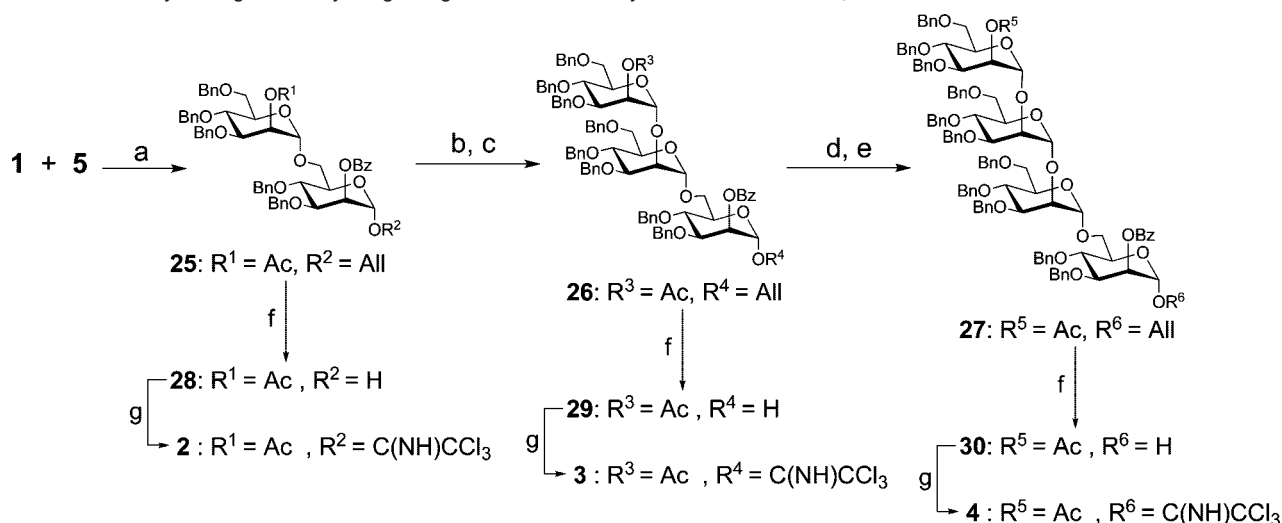
(39) Kwon, Y. U.; Soucy, R. L.; Snyder, D. A.; Seeberger, P. H. *Chem. – Eur. J.* **2005**, *11*, 2493–2504.

(40) Cid, M. B.; Alfonso, F.; Martin-Lomas, M. *Synlett* **2003**, 1370–1372.

(41) Liu, X.; Seeberger, P. H. *Chem. Commun.* **2004**, 1708–1709.

(42) Vishwakarma, R. A.; Menon, A. K. *Chem. Commun.* **2005**, 453–455.

(43) Liu, X.; Kwon, Y. U.; Seeberger, P. H. *J. Am. Chem. Soc.* **2005**, *127*, 5004–5005.

Scheme 6. Assembly of Oligomannosylating Reagents 2–4 for the Synthesis of **PIM**₄–**PIM**₆^a

^a Reagents and conditions: (a) TMSOTf, CH₂Cl₂, −10 °C, quant.; (b) AcCl, MeOH, CH₂Cl₂, 0 °C, 91%; (c) **1**, TMSOTf, −40 °C, Toluene, 95%; (d) AcCl, MeOH, CH₂Cl₂, 0 °C, 84%; (e) **1**, TMSOTf, Toluene, −40 °C, 96%; (f) Pd(OAc)₂, MeOH, PPh₃, Et₂NH, 77% for **28**, 95% for **29**, and 83% for **30**; (g) Cl₃CCN, NaH, rt, 85% for **2**, 86% for **3**, and 89% for **4**.

conserved pathogenic structures that are secreted or exposed on the surface of viruses or bacteria.^{46,48–50} Upon binding to DC-SIGN, the antigens are internalized, processed and later presented on the surface of dendritic cells together with costimulatory molecules.^{51,52} Mycobacteria also use DC-SIGN as a receptor to enter dendritic cells.⁵¹

Glass slides printed with the immobilized **PI** and **PIM**₁–**PIM**₆ were incubated with a DC-SIGN solution in buffer at room temperature to allow DC-SIGN to bind to the immobilized PIMs. Excess DC-SIGN was washed off and bound DC-SIGN was detected by incubation with a fluorescein-conjugated anti-DC-SIGN antibody. The difference in DC-SIGN binding affinity to the synthetic PIM compounds was assessed semiquantitatively by monitoring the fluorescence intensity via a fluorescence scanner (for fluorescent intensity data, see Supporting Information). Synthetic PIMs bind to DC-SIGN in a specific manner (Figure 3). Although both synthetic analogs of the most abundant **PIM**₂ and **PIM**₆ are recognized by DC-SIGN, the larger synthetic oligosaccharides **PIM**₅ and **PIM**₆ bound to DC-SIGN to a greater extent. This observation underlines the significance of the α-1,2- mannose motif present in both PIMs and ManLAM structures.⁵³

Adjuvant Activity of PIMs. An important feature of natural PIMs is their ability to induce a host cell immune response. To investigate immunostimulatory effects of these synthetic PIMs

four C57BL/6 mice per group were prime-boost immunized with the model antigen keyhole-limpet hemocyanin (KLH) covalently linked to **PIM**₆. As expected, immunization with the pure antigen KLH resulted in detectable anti-KLH antibody levels. Antibody production in the presence of the well-established adjuvants Freund's adjuvant, alum and CpG, increased substantially. In comparison, conjugation of **PIM**₆ glycan to KLH also resulted in a marked increase of anti-KLH antibodies that was statistically significant for each serum dilution compared to KLH alone (Figure 4A). To address the mechanism causing the increased antibody production after covalent attachment of **PIM**₆ to KLH, we restimulated spleen cells of immunized mice with KLH *ex vivo* and measured proliferation. Spleen cell proliferation of mice that had been immunized with KLH–**PIM**₆ was significantly increased indicating that T cell priming was stimulated by **PIM**₆ glycan (Figure 4B). It is also known that adjuvant properties not only depend on antibody production and T cell proliferation, but also on other T effector functions such as cytokine production. To this end, we measured IFN-γ production of T cells by ELISpot analysis. The frequency of IFN-γ producing T cells in spleen was determined upon restimulation of T cells with KLH. The ability of T cells to produce IFN-γ was increased in spleen cells of mice that had been immunized with KLH–**PIM**₆ conjugate (Figure 4C). The effect was even stronger than with the well-established adjuvants Freund's adjuvant, alum or CpG, which highlights the immunostimulatory capacity of synthetic **PIM**₆ glycan. Concanavalin A was used as a positive control since it serves as a T cell mitogen and stimulates all T cells to the same extent.

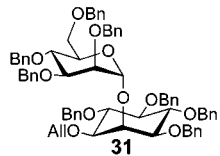
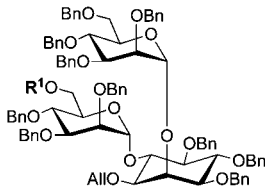
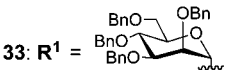
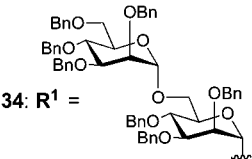
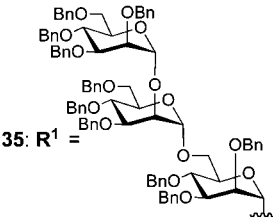
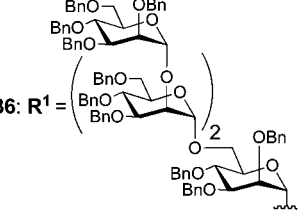
Recognition of **PIM**₆ by pattern recognition receptors on antigen-presenting cells might provide a danger signal, thereby facilitating enhanced uptake of the model antigen and increased expression of costimulatory molecules. The effect of **PIM**₆ on T cell proliferation and T cell effector functions such as IFN-γ production clearly indicates that antigen presentation by APCs and T cell activation are increased by **PIM**₆ glycan.

The synthetic **PI** and **PIM**₅–**PIM**₆ described here will be suitable for conjugation with other appropriate surfaces such as fluorescent nanocrystals, beads or fluorophores to generate probes for cellular assays. Such tools may shed light on the mechanism

- (44) de Paz, J. L.; Horlacher, T.; Seeberger, P. H. *Methods Enzymol.* **2006**, *415*, 269–292.
- (45) van Kooyk, Y.; Geijtenbeek, T. B. *Nat. Rev. Immunol.* **2003**, *3*, 697–709.
- (46) Cambi, A.; Figdor, C. G. *Curr. Opin. Cell Biol.* **2003**, *15*, 539–546.
- (47) Banchereau, J.; Steinman, R. M. *Nature* **1998**, *392*, 245–252.
- (48) Cambi, A.; Koopman, M.; Figdor, C. G. *Cell. Microbiol.* **2005**, *7*, 481–488.
- (49) Su, S. V.; Hong, P.; Baik, S.; Negrete, O. A.; Gurney, K. B.; Lee, B. *J. Biol. Chem.* **2004**, *279*, 19122–19132.
- (50) Geijtenbeek, T. B.; Engering, A.; Van Kooyk, Y. *J. Leukoc. Biol.* **2002**, *71*, 921–931.
- (51) De Libero, G.; Mori, L. *Nat. Rev. Immunol.* **2005**, *5*, 485–496.
- (52) De Libero, G.; Mori, L. *FEBS Lett.* **2006**, *580*, 5580–5587.
- (53) Koppel, E. A.; Ludwig, I. S.; Hernandez, M. S.; Lowary, T. L.; Gadikota, R. R.; Tuzikov, A. B.; Vandenbroucke-Grauls, C. M.; van Kooyk, Y.; Appelmel, B. J.; Geijtenbeek, T. B. *Immunobiology* **2004**, *209*, 117–127.

Table 2. Assembly of Fully Protected **PIM**₁–**PIM**₆ Backbones: Union of (oligo)Mannosyl Fragment (**X**) and Inositol-Containing Pseudosaccharide Fragment (**Y**)

a) Glycosylation (except entry 2)
 b) NaOMe / MeOH, 50 °C, 24 h
 c) BnBr, NaH, 0 °C to rt, 12 h

Entry	X	Y	Glycosylation Conditions	Products	Yields a) ; b) ; c)
1	1	23	TMSOTf, -40 °C, Et ₂ O	 31	a) 69%; b) and c) quant. (2 steps)
2	not applied	8	No Glycosylation	 32: R¹ = Bn	b) and c) 90% (2 steps)
3	1	8	TMSOTf, -10 °C, CH ₂ Cl ₂	 33: R¹ =	a), b), and c) 89% (3 steps)
4	2	8	TMSOTf, -10 °C, CH ₂ Cl ₂	 34: R¹ =	a), b), and c) 89% (3 steps)
5	3	8	TMSOTf, -10 °C, CH ₂ Cl ₂	 35: R¹ =	a), b), and c) 73% (3 steps)
6	4	8	TMSOTf, 0 °C, CH ₂ Cl ₂	 36: R¹ =	a) 64%; b) and c) 97% (2 steps)

by which PIM structures on *Mtb* can influence bacterial trafficking in host cells. The synthetic compounds can also be attached to affinity columns in search for proteins or enzymes in cell lysates that interact with PIMs. Moreover, the synthetic PIMs can be used as substrates to explore biosynthetic pathways of the PIMs.

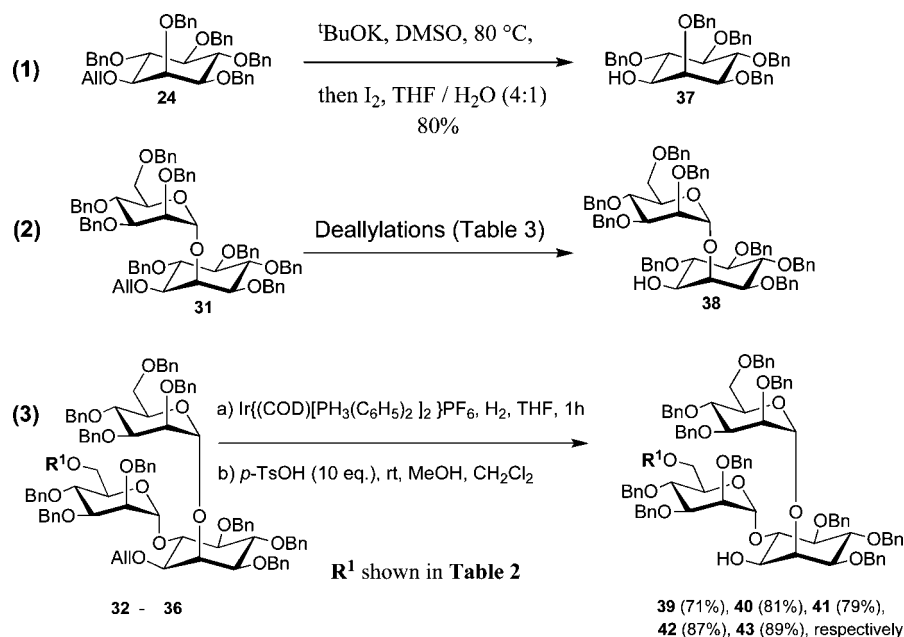
We are investigating the possibility of applying synthetic PIMs as antigens to elicit an immune response against *Mtb* as well as their adjuvant properties *in vivo*. For these purposes, the synthetic compounds can be conjugated to different model antigens.

Conclusion

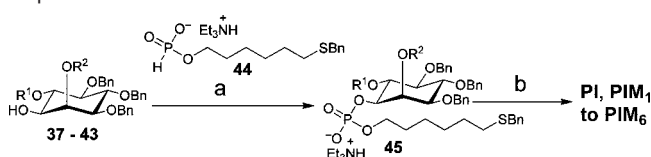
In this study, the efficient synthesis of all PIMs including phosphatidylinositol (**PI**) and **PIM**₁ to **PIM**₆ was reported. A

robust and practical synthesis to the PIM molecules was developed utilizing mannosyl bicyclic and tricyclic orthoesters and mannosyl phosphates. The key intermediate orthoesters allowed for rapid and scalable syntheses of mannoside building blocks and the glycosylations of the mannosyl phosphates resulted in excellent yields and stereoselectivity. All synthetic PIMs are equipped with a thiol linker to be readily immobilized on microarray surfaces. Thus, the synthetic PIMs represent tools for various biological studies. An application of the synthetic **PI** and **PIMs** for interaction with the protein DC-SIGN was

(54) Takahashi, H.; Kittaka, H.; Ikegami, S. *J. Org. Chem.* **2001**, *66*, 2705–2716.

Scheme 7. Removal of Allyl Protecting Groups on C1 *myo*-Inositol of Fully Protected **PI** and **PIM₂–PIM₆****Table 3.** Removal of Allyl Protecting Group on Pseudo-Disaccharide **31**

entry	conditions	yield
1	^t BuOK, DMSO, 80 °C, then I ₂ , THF/H ₂ O TMSOTf	10%, (decomposition)
2	Pd(OAc) ₂ , PPh ₃ , HNEt ₂ , CH ₂ Cl ₂ /MeOH (2:1)	no reaction
3	[Ir(COD)(PCH ₃ Ph ₂) ₂]PF ₆ (cat.), H ₂ , THF then I ₂ in THF/H ₂ O (2:1)	30%
4	[Ir(COD)(PCH ₃ Ph ₂) ₂]PF ₆ (cat.), H ₂ , THF then <i>p</i> -TsOH (cat.) in DCM/MeOH (1:3)	quantitative

Scheme 8. Phosphorylation of Oligosaccharides **37–43** and Global Deprotection under Birch Reduction Conditions^a

^a Reagents and conditions: (a) i. **44**, PivCl, pyridine, ii. I₂, H₂O, pyridine, 90% to quant., 2 steps; (b) i. Na/NH₃ (l) *t*-BuOH, -78 °C, ii. MeOH, 65% for **PI**, 43% for **PIM₁**, 56% for **PIM₂**, 91% for **PIM₃**, 65% for **PIM₄**, 88% for **PIM₅**, and 84% for **PIM₆**.

demonstrated. The difference in DC-SIGN binding affinity among synthetic **PI** and **PIM** compounds was observed in a specific manner. Immunization experiments in mice revealed the potential of synthetic **PIMs** to serve as immune stimulators.

Experimental Section

Immunization of Mice and Detection of anti-KLH Antibody Levels in Sera. Preparation of keyhole limpet hemocyanin (KLH) in complete/incomplete Freund's adjuvant was performed by mixing KLH with Freund's adjuvant in a 1:1 volume ratio. For coupling of **PIM₆** to KLH, **PIM₆** was incubated with Tris(2-carboxyethyl)phosphine HCl (TCEP) in equal molar ratio for one hour at rt. A molar excess of **PIM₆** was then coupled to KLH using the Inject Maleimide Activated mKLH Kit (Pierce, Rockford, IL) according to manufacturer's instructions. **PIM₆**–KLH conjugate was purified by gel filtration chromatography and the

protein concentration in the eluate was determined by measuring the absorption at a wavelength of 280 nm.

Female C57BL/6 mice (6–8 weeks old) were housed in the HCl rodent center, ETH Zürich, and were provided food and water *ad libitum*. On day 0 four mice per group were *s.c.* immunized with KLH alone (group 1), KLH in complete Freund's adjuvant (group 2), KLH with alum (group 3), KLH with CpG (group 4) or KLH coupled to **PIM₆** (group 5). On day 10, mice received a boost immunization with KLH alone (group 1), KLH in incomplete Freund's adjuvant (group 2), KLH with alum (group 3), KLH with CpG (group 4) or KLH coupled to **PIM₆** (group 5). The amount of KLH was adjusted to 50 µg per mouse and immunization. On day

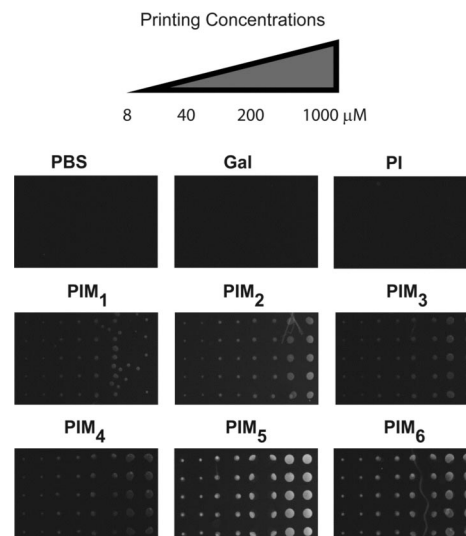


Figure 3. Fluorescent scanning of **PIM** microarray incubated with DC-SIGN and subsequently with fluorescein conjugated antihuman DC-SIGN antibody (1 h). A **PI** and **PIM** immobilized glass slide was incubated with a solution of DC-SIGN (1 µg/100 µL) in HEPES buffer containing 1% BSA, 20 mM CaCl₂, and 0.5% Tween-20 at room temperature for 1 h. The slide was washed thoroughly and incubated with a solution of fluorescein conjugated antihuman DC-SIGN antibody (0.5 µg/100 µL) in HEPES buffer containing 1% BSA and 0.5% Tween-20 at room temperature for 1 h. The slide was washed thoroughly and scanned by a fluorescent microarray scanner. (PBS = Phosphate-buffered saline, Gal = Galactose)

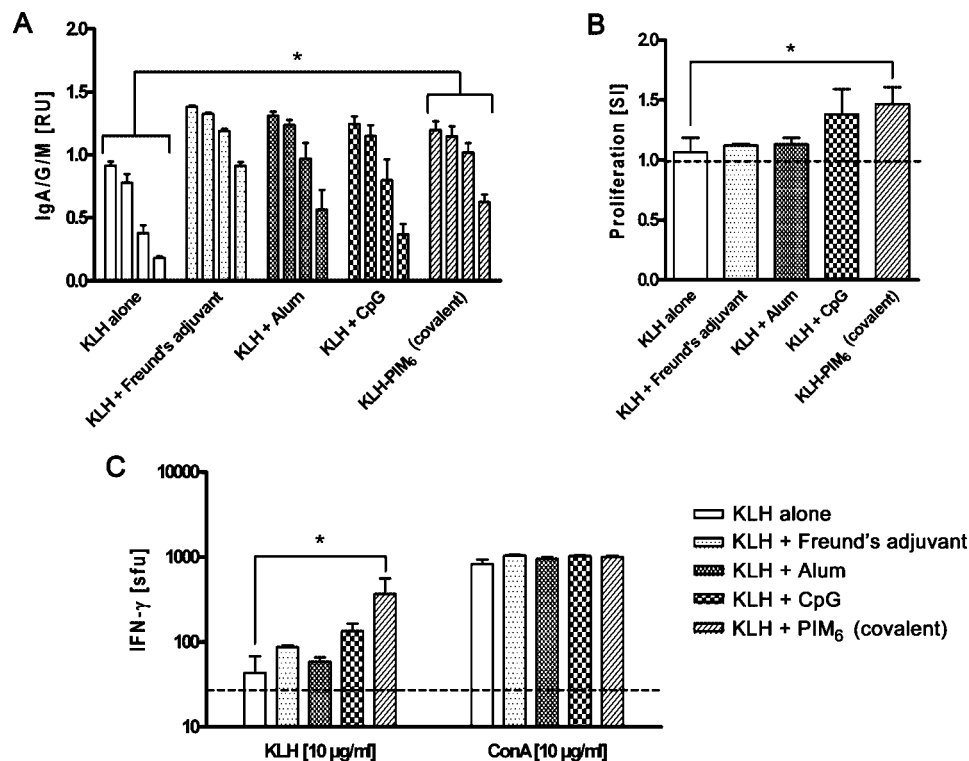


Figure 4. Immunization studies in mice with the model antigen KLH coupled to PIM₆. On day 0, four C57BL/6 mice per group (6–8 weeks) were s.c. immunized with KLH alone, KLH in complete Freund's adjuvant, KLH with alum, KLH with CpG or KLH covalently linked to PIM₆. On day 10, mice received a boost immunization with KLH alone, KLH in incomplete Freund's adjuvant, KLH with alum, KLH with CpG, or KLH–PIM₆. (A) On day 17 post immunization blood was taken from the saphenous vein of the immunized mice and levels of anti-KLH antibodies (sum of IgA, IgG and IgM) were measured by ELISA in serial dilutions of the sera (1:1000, 1:2000, 1:10000, 1:50000, duplicates for each mouse). Data are presented as mean \pm SEM for each group of mice. Statistical analysis was performed with Student's *t* test (*, $p < 0.05$). (B) On day 20 post immunization, 2×10^5 splenocytes were restimulated with KLH (10 μ g/ml) for 24 h and cell proliferation was measured. The results are expressed as a stimulation index (SI) which is the net proliferation of spleen cell cultures stimulated with 10 μ g/ml KLH divided by the net proliferation of spleen cell cultures in medium. Data are presented as mean \pm SEM for each group of mice. Statistical analysis was performed with Student's *t* test (*, $p < 0.05$). The dashed line represents proliferation of spleen cells from unimmunized mice. (C) On day 20, 2×10^5 splenocytes were stimulated with KLH (10 μ g/ml) or Concanavalin A (ConA, 10 μ g/ml) in a 96-Well plate coated with antimouse-IFN- γ and the frequency of IFN- γ producing cells was determined by ELISpot analysis. The results are expressed as spot forming units (sfu) which is the number of cells producing IFN- γ in each well. Data are presented as mean \pm SEM for each group of mice. Statistical analysis was performed with Student's *t* test (*, $p < 0.05$). The dashed line represents IFN- γ production of cells cultivated in medium (unspecific background).

17, blood was taken from the saphenous vein and serum was separated from the clotted blood by centrifugation. All animal experiments were in accordance with local Animal Ethics Committee regulations.

Levels of anti-KLH antibodies in sera of immunized mice were measured by ELISA. Briefly, Microtiter microplates (Greiner, Frickenhausen, Germany) were coated with 10 μ g/mL KLH in 0.05 M Na₂CO₃ buffer (pH 9.6) at 4 $^{\circ}$ C overnight. After blocking with 1% BSA/PBS for two hours at rt and washing with 0.05% Tween-20/PBS plates were incubated with serial dilutions of sera (diluted in 0.1% BSA/PBS) for two hours. Plates were then washed three times with 0.05% Tween-20/PBS and incubated with HRP-conjugated goat-antimouse IgG+A+M antibody in a dilution of 1:1000 (Invitrogen, Basel, Switzerland). Detection was performed by using the 3,3',5,5'-Tetramethylbenzidine Liquid Substrate System (Sigma-Aldrich, Buchs, Switzerland) according to manufacturer's instructions.

T Cell Proliferation and ELISpot Analysis. On day 20 after the first immunization, mice were sacrificed and spleens were removed. RBCs were lysed by adding hypotonic ammonium chloride solution. Single cell suspensions were cultivated at 2×10^5 cells per well in 96-well plates for 24 h in the presence of medium or KLH (10 μ g/mL) for restimulation of T cells *ex vivo*. Proliferation of spleen cells was measured using the CellTiter 96 Aqueous One Solution Cell Proliferation Assay (Promega, Madison, WI) according to the manufacturer's instructions.

ELISpot analysis was performed on day 20 after the first immunization using a mouse IFN- γ ELISpot Kit (R&D Systems, Minneapolis, MN). Briefly, 2×10^5 spleen cells per well were stimulated for 24 h in the presence of medium, KLH (10 μ g/mL) or the T cell mitogen concanavalin A (ConA, 10 μ g/mL). Spot development was performed according to the manufacturer's instructions and the number of spots was determined using an ELISpot reader (AID, Straussberg, Germany).

Statistical Analysis. Statistical analyses were performed applying unpaired Student's *t* test. All statistical analyses were performed with the Prism software (Graph Pad Software, San Diego, CA).

Acknowledgment. This research was supported by ETH Zürich, the Swiss National Science Foundation (SNF Grant 200121-101593), and the Roche Research Foundation (postdoctoral fellowship for S.B.). S.B. thanks Thailand Research Fund for financial support.

Supporting Information Available: Complete synthetic procedures, NMR spectral copies of all new compounds and complete ref 21. This material is available free of charge via the Internet at <http://pubs.acs.org>.

JA806283E